MFEM APPLICATION TO EM-WAVE SIMULATION IN ECR SPACE PLASMA THRUSTERS

Alvaro Sánchez Villar

Email: asanche2@pppl.gov

ONERA

THE FRENCH AEROSPACE LAB

uc3m

PPPL

Special acknowledgements to:

Mario Merino, Eduardo Ahedo, Jiewei Zhou & Adrián Dominguez-Vazquez (Universidad Carlos III de Madrid)

Federico Boni, Victor Desangles, Julien Jarrige and Denis Packan (ONERA)

Syun'ichi Shiraiwa and Nicola Bertelli (PPPL)

CONTENTS

1. Background
    a. Electric propulsion
    b. Electron Cyclotron Resonance Thrusters
2. ATHAMES
3. Coupled ECRT Simulations
4. Validation
5. Petra-M preliminary results
6. Conclusions

BACKGROUND

- Electric propulsion (EP)
  - More efficient use of propellant in space compared to chemical propulsion.
  - Most mature electric propulsion technologies (e.g. Hall Effect Thruster, Gridded Ion Thruster) incorporate electrodes: Erosion → impact on thruster lifetime
- Electrodeless plasma thrusters (EPTs)
  - EPTs operation based on radiofrequency coupling :
    - VASIMR
    - Helicon plasma thruster (HPT)
    - Electron Cyclotron Resonance Thruster (ECRT)

HALL EFECT THRUSTER (SEP-NASA)

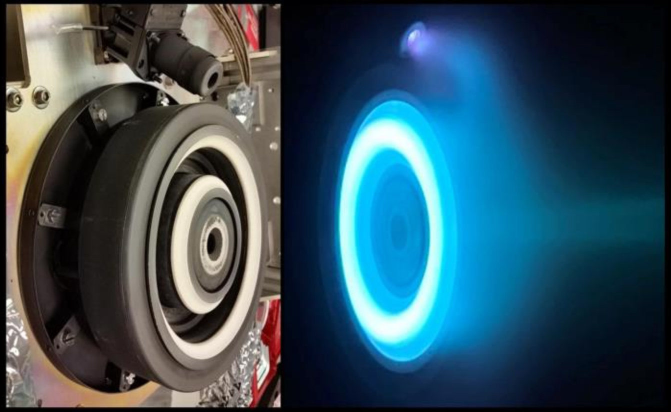

VASIMR (AARC)

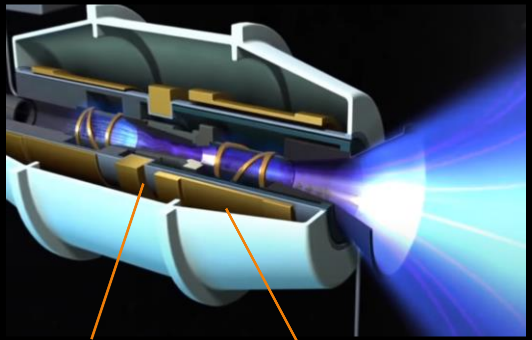

HPT(UC3M)

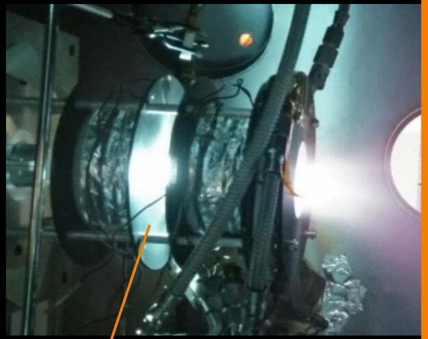

ECRT (ONERA)

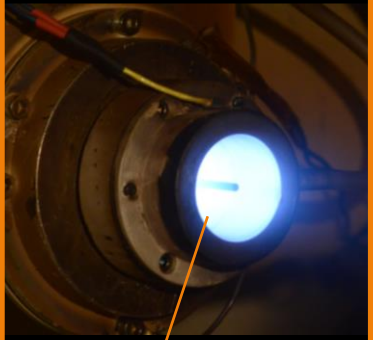

ECRT OPERATION

- Electron Cyclotron Resonance (ECR):
  - Electrons cyclotron motion resonates with electromagnetic (EM) waves whenever their frequencies match as:

$$\omega_{ce} = \frac{eB}{m_e} = \omega$$

- Energized electrons ionize the propellant injected
- Electrons accelerate along the Magnetic nozzle expansion
- An electrostatic potential develops, which accelerates the ions

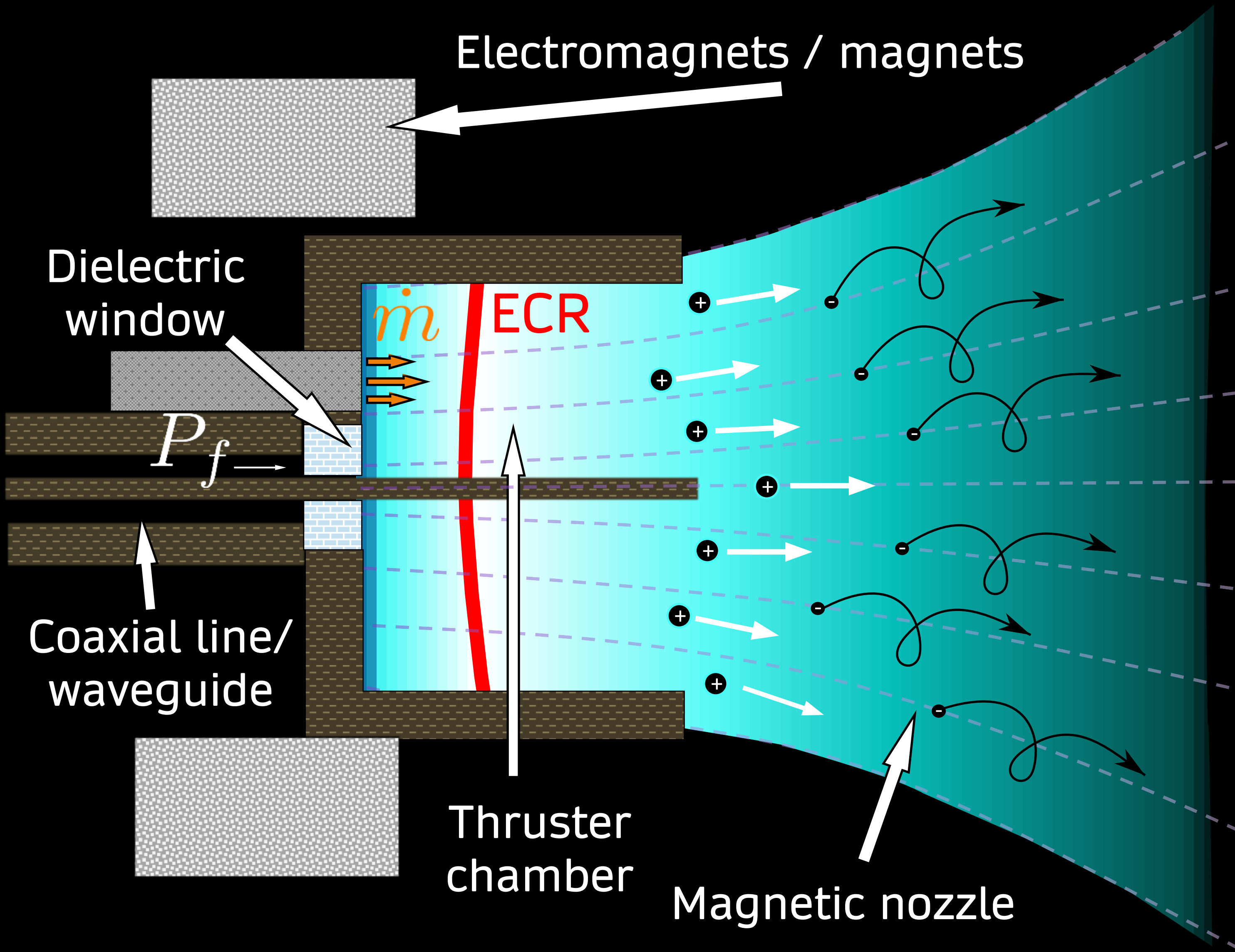

ATHAMES

- Axisymmetric Time HArmonic Maxwell’s Equations Solver (ATHAMES)
  - Solves Maxwell’s inhomogeneous wave equation in weak form 2D axisymmetric.
  - Finite element method based on a mixed basis formulation.
  - Coded in C++; use of MFEM FE discretization library:
    - Also used by Petra-M analyzing the EM waves in the scrap off layer of a tokamak.
  - Inhomogeneous anisotropic permittivity tensor.
  - Boundary conditions:
    - Perfect electric conductor (PEC).
    - Perfect magnetic conductor (PMC).
    - Symmetry axis.
  - Unstructured grids (GMSH):
    - Complex geometries (e.g., curved).
    - Non-uniform meshes.
    - Predictive mesh refinement.

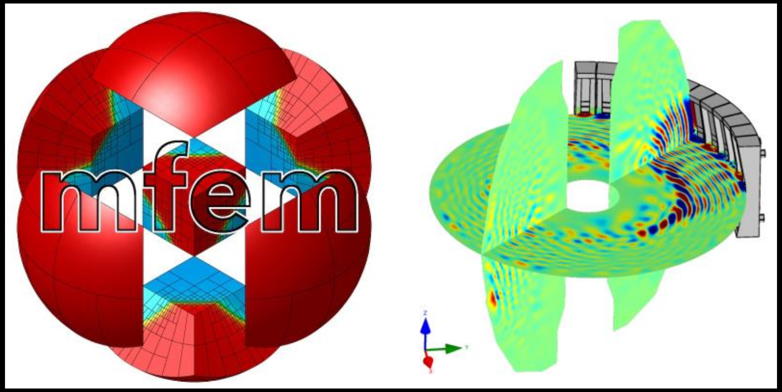

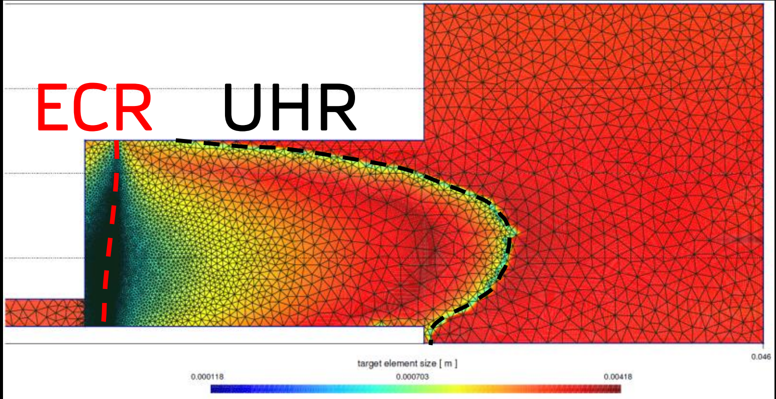

ATHAMES

- Mathematical formulation (weak form) after boundary conditions:

$$\nabla \times \nabla \times \hat{\boldsymbol{E}} - \frac{\omega^2}{c^2}\bar{\bar{\kappa}} \cdot \hat{\boldsymbol{E}} = i\omega\mu_0 \hat{\boldsymbol{j}}_a \rightarrow \iiint_\Omega \left[\left(\nabla \times \hat{\boldsymbol{W}}^*\right) \cdot \left(\nabla \times \hat{\boldsymbol{E}}\right) - k_0^2 \left(\bar{\bar{\kappa}}\hat{\boldsymbol{E}}\right) \cdot \hat{\boldsymbol{W}}^*\right] \mathrm{d}V = i\mu_0\omega \iiint_\Omega \hat{\boldsymbol{W}}^* \cdot \hat{\boldsymbol{j}}_a \mathrm{d}V\,.$$

  - $\hat{\boldsymbol{W}}$ and $\hat{\boldsymbol{E}}$ chosen following Galerkin method.
- Harmonic expansion in azimuthal direction

$$\hat{\boldsymbol{E}}(z,r,\theta) = \sum_{m=-\infty}^{\infty} \tilde{\boldsymbol{E}}^{(m)}(z,r)e^{im\theta}\,,$$

$$\hat{\boldsymbol{j}}_a(z,r,\theta) = \sum_{m=-\infty}^{\infty} \tilde{\boldsymbol{j}}_a^{(m)}(z,r)e^{im\theta}\,.$$

- Mixed FE discretization

$$\tilde{\boldsymbol{E}}(x_1,x_2) = \sum_i a_i \tilde{\boldsymbol{N}}_i(x_1,x_2) + \sum_l b_l \tilde{L}_l(x_1,x_2)\mathbf{1}_{x_3}\,,$$

  - In-plane: Nédélec vector elements ($\tilde{\boldsymbol{N}}_i$)

$$\tilde{\boldsymbol{N}}_i = l_{ij}\left(\lambda_i \nabla \lambda_j - \lambda_j \nabla \lambda_i\right)$$

  - Out-of-plane: Lagrange nodal elements $\tilde{L}_i$
    - Polynomial order p_L

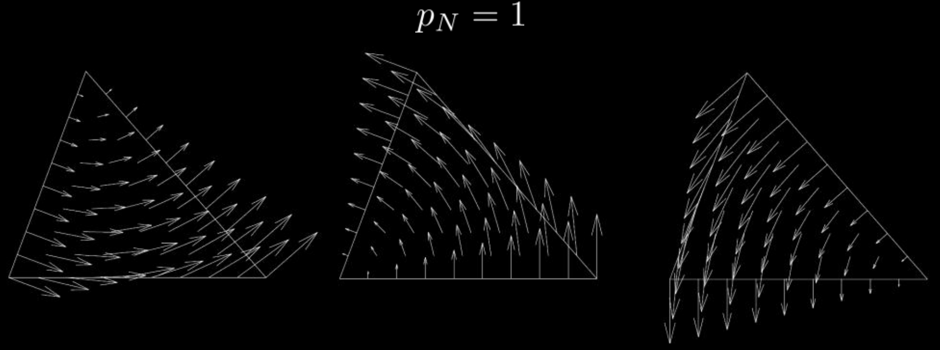

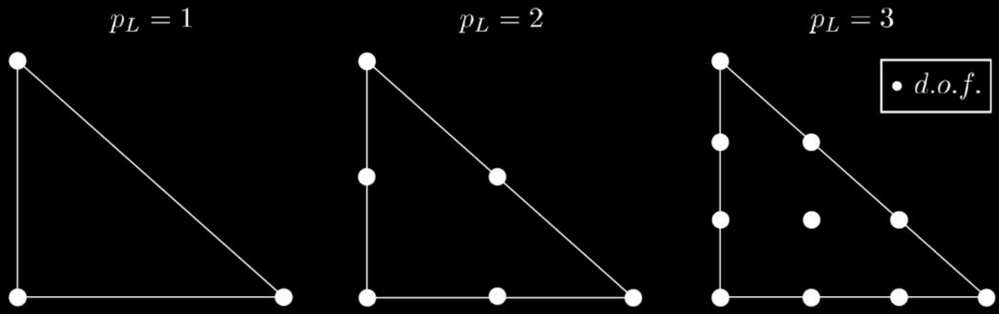

- Block matrix assembly (A)

	$\tilde{\boldsymbol{E}}_t^R$	$\tilde{\boldsymbol{E}}_t^I$	$\tilde{E}_\theta^R$	$\tilde{E}_\theta^I$
$\tilde{\boldsymbol{W}}_t^R$	$r\,(\nabla\times\tilde{\boldsymbol{W}}_t^R)\cdot(\nabla\times\tilde{\boldsymbol{E}}_t^R)$ $-rk_0^2(\bar{\bar{\kappa}}_{t,t}^R\cdot\tilde{\boldsymbol{E}}_t^R)\cdot\tilde{\boldsymbol{W}}_t^R$ $+\frac{m^2}{r}\tilde{\boldsymbol{E}}_t^R\cdot\tilde{\boldsymbol{W}}_t^R$	$rk_0^2(\bar{\bar{\kappa}}_{t,t}^I\cdot\tilde{\boldsymbol{E}}_t^I)\cdot\tilde{\boldsymbol{W}}_t^R$	$-rk_0^2\tilde{E}_\theta^R\boldsymbol{\kappa}_{t,\theta}^R\cdot\tilde{\boldsymbol{W}}_t^R$	$-\frac{m}{r}\nabla(r\tilde{E}_\theta^I)\cdot\tilde{W}_t^R$ $+rk_0^2\tilde{E}_\theta^I\boldsymbol{\kappa}_{t,\theta}^I\cdot\tilde{\boldsymbol{W}}_t^R$
$\tilde{\boldsymbol{W}}_t^I$	$-rk_0^2\left[\bar{\bar{\kappa}}_{t,t}^I\cdot\tilde{\boldsymbol{E}}_t^R\right]\cdot\tilde{\boldsymbol{W}}_t^I$	$r\,(\nabla\times\tilde{\boldsymbol{W}}_t^I)\cdot(\nabla\times\tilde{\boldsymbol{E}}_t^I)$ $-rk_0^2\left[\bar{\bar{\kappa}}_{t,t}^R\cdot\tilde{\boldsymbol{E}}_t^I\right]\cdot\tilde{\boldsymbol{W}}_t^I$ $+\frac{m^2}{r}\tilde{\boldsymbol{E}}_t^I\cdot\tilde{\boldsymbol{W}}_t^I$	$\frac{m}{r}\nabla(r\tilde{E}_\theta^R)\cdot\tilde{W}_t^I$ $-rk_0^2\tilde{E}_\theta^R\boldsymbol{\kappa}_{t,\theta}^I\cdot\tilde{\boldsymbol{W}}_t^I$	$-rk_0^2\tilde{E}_\theta^I\boldsymbol{\kappa}_{t,\theta}^R\cdot\tilde{\boldsymbol{W}}_t^I$
$\tilde{W}_\theta^R$	$-rk_0^2\tilde{W}_\theta^R\boldsymbol{\kappa}_{\theta,t}^R\cdot\tilde{\boldsymbol{E}}_t^R$	$\frac{m}{r}\nabla(r\tilde{W}_\theta^R)\cdot\tilde{\boldsymbol{E}}_t^I$ $+rk_0^2\tilde{W}_\theta^R\boldsymbol{\kappa}_{\theta,t}^I\cdot\tilde{\boldsymbol{E}}_t^I$	$\frac{1}{r}\nabla(r\tilde{W}_\theta^R)\cdot\nabla(r\tilde{E}_\theta^R)$ $-rk_0^2\kappa_{\theta\theta}^R\ \tilde{E}_\theta^R\tilde{W}_\theta^R$	$rk_0^2\kappa_{\theta\theta}^I\tilde{E}_\theta^I\tilde{W}_\theta^R$
$\tilde{W}_\theta^I$	$-\frac{m}{r}\nabla(r\tilde{W}_\theta^I)\cdot\tilde{\boldsymbol{E}}_t^R$ $-rk_0^2\tilde{W}_\theta^I\boldsymbol{\kappa}_{\theta,t}^I\cdot\tilde{\boldsymbol{E}}_t^R$	$-rk_0^2\tilde{W}_\theta^I\boldsymbol{\kappa}_{\theta,t}^R\cdot\tilde{\boldsymbol{E}}_t^I$	$-rk_0^2\kappa_{\theta,\theta}^I\tilde{E}_\theta^R\tilde{W}_\theta^I$	$\frac{1}{r}\nabla(r\tilde{W}_\theta^I)\cdot\nabla(r\tilde{E}_\theta^I)$ $-rk_0^2\kappa_{\theta,\theta}^R\ \tilde{E}_\theta^I\tilde{W}_\theta^I$

ATHAMES

- Axisymmetric boundary conditions

$$E_r^{(0)} = E_\theta^{(0)} = 0\,,$$
$$E_r^{(\pm 1)} = \mp i E_\theta^{(\pm 1)} = 0\,, \quad E_z^{(\pm 1)} = 0\,,$$
$$E_r^{(m)} = E_\theta^{(m)} = E_z^{(m)} = 0\,, \quad |m| > 1\,.$$

- Discretization dependent on mode number

$$\boldsymbol{E}^{(m)} = \begin{cases} \sum_{i=1}^{N_\mathrm{edge}} \boldsymbol{N}_i\,(r,z)\, e_{t,i}^{(m)} + \mathbf{1}_\theta \sum_{i=1}^{N_\mathrm{node}} N_i\,(r,z)\, e_{\theta,i}^{(m)}\,, & m = 0\,, \\ \sum_{i=1}^{N_\mathrm{edge}} r\boldsymbol{N}_i\,(r,z)\, e_{t,i}^{(m)} + (\mathbf{1}_\theta \mp i\mathbf{1}_r) \sum_{i=1}^{N_\mathrm{node}} N_i\,(r,z)\, e_{\theta,i}^{(m)}\,, & m = \pm 1\,, \\ \sum_{i=1}^{N_\mathrm{edge}} r\boldsymbol{N}_i\,(z,r)\, e_{t,i}^{(m)} + \mathbf{1}_\theta \sum_{i=1}^{N_\mathrm{node}} N_i\,(z,r)\, e_{\theta,i}^{(m)}\,, & |m| > 1\,. \end{cases}$$

- Combined with PEC boundary conditions on the azimuthal fields at the symmetry axis.

- Code verification using:
  - The Method of Manufactured solutions
    - Manufactured solution

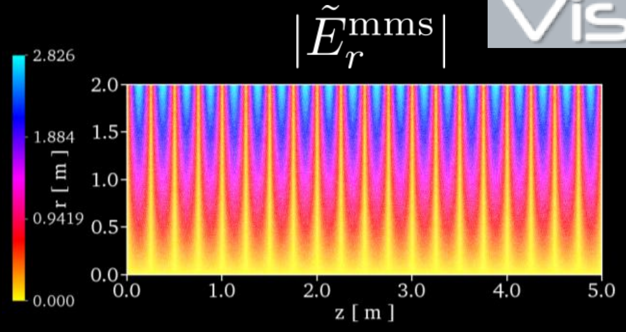

$$
\begin{cases}
\tilde{E}_z^{\mathrm{mms}} &= \sin(k_1 r) + i\sin(k_2 r)\ ,\\
\tilde{E}_r^{\mathrm{mms}} &= r\left[\sin(k_1 z) + i\sin(k_2 z)\right]\ ,\\
\tilde{E}_\theta^{\mathrm{mms}} &= \sin(k_1 r) + i\sin(k_2 r)\ .
\end{cases}
$$

$$\nabla\times\nabla\times\tilde{\boldsymbol{E}}^{\mathrm{mms}} - \frac{\omega^2}{c^2}\bar{\bar{\kappa}}\cdot\tilde{\boldsymbol{E}}^{\mathrm{mms}} = i\omega\mu_0\tilde{\boldsymbol{j}}_a^{\mathrm{mms}} \longrightarrow \tilde{\boldsymbol{j}}_a^{\mathrm{mms}}$$

ATHAMES

$\tilde{\boldsymbol{E}}$

$$e = \int_\Sigma \|\tilde{\boldsymbol{E}} - \tilde{\boldsymbol{E}}^{\mathrm{mms}}\|_2 d\Sigma$$

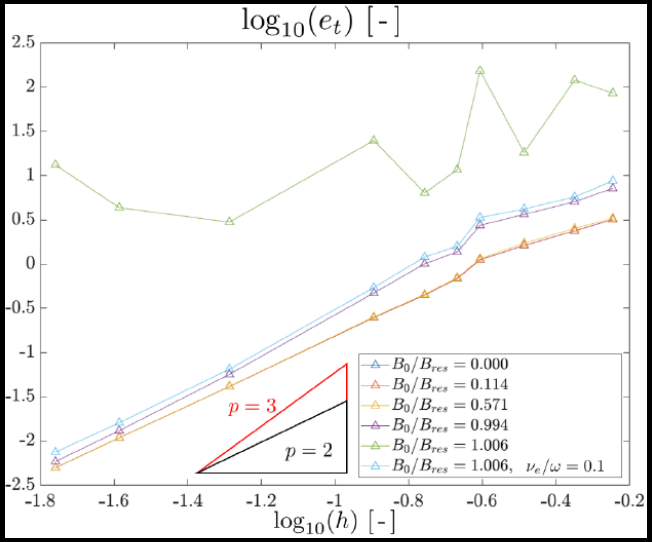

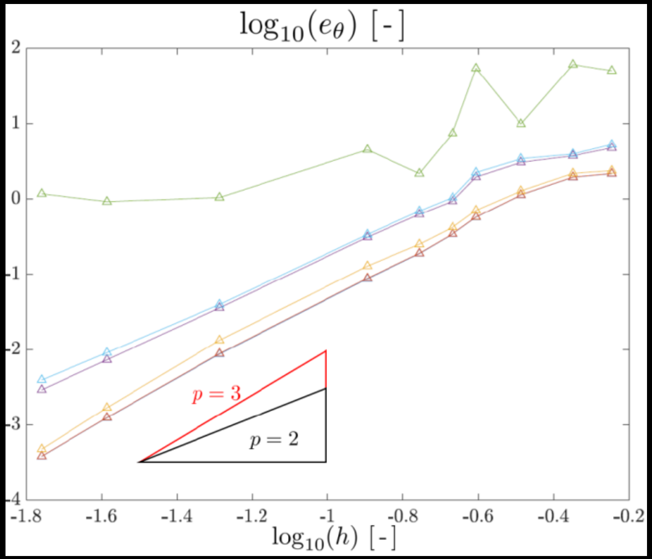

  - Error convergence agreement with FE order used
    - Tangential fields (vector) order 2
    - Azimuthal fields (nodal) order 3

- Predictive mesh refinement
  - Fast oscillations in specific CMA regions
    - Similar oscillations observed in other research for the lower hybrid resonance (LHR) in the context of fusion.
  - Spurious character since fast oscillations wavelength is much smaller tan physical, and in the order of the mesh characteristic length.
  - Predictive refinement allows to mitigate these oscillations from the solution.

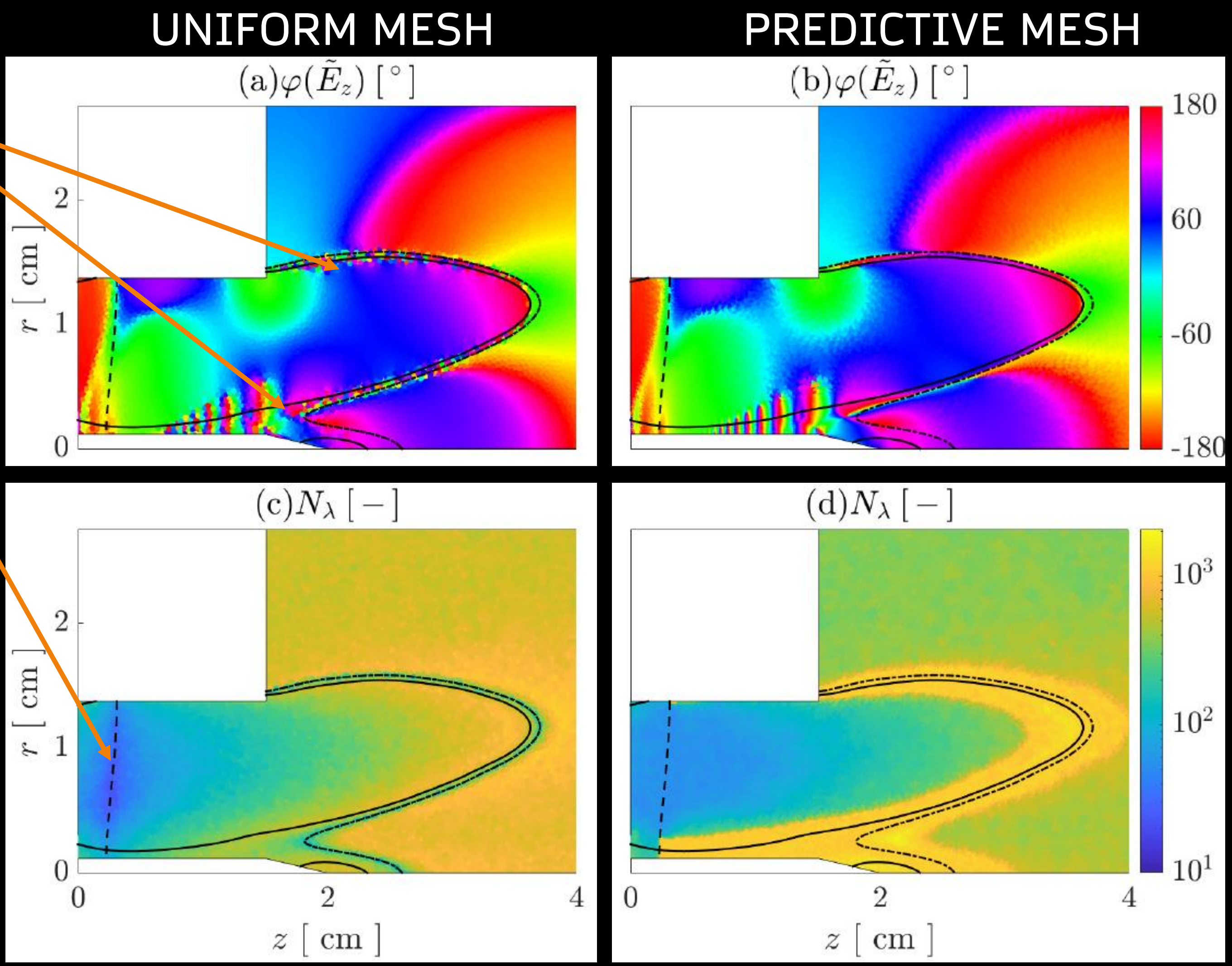

COUPLED ECRT SIMULATION

PLASMA TRANSPORT

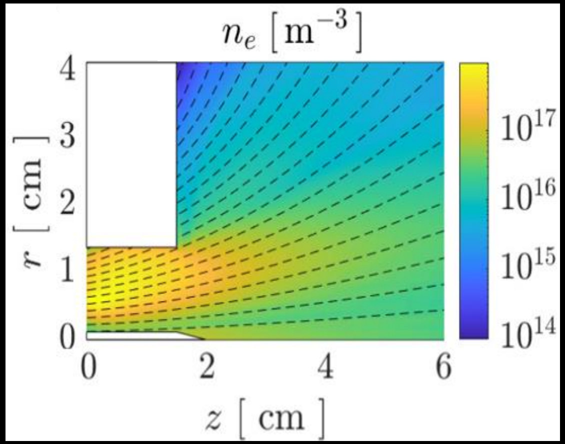

ELECTROMAGNETIC RESPONSE

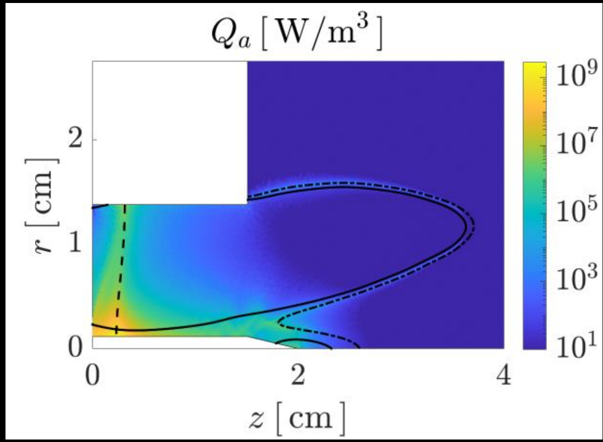

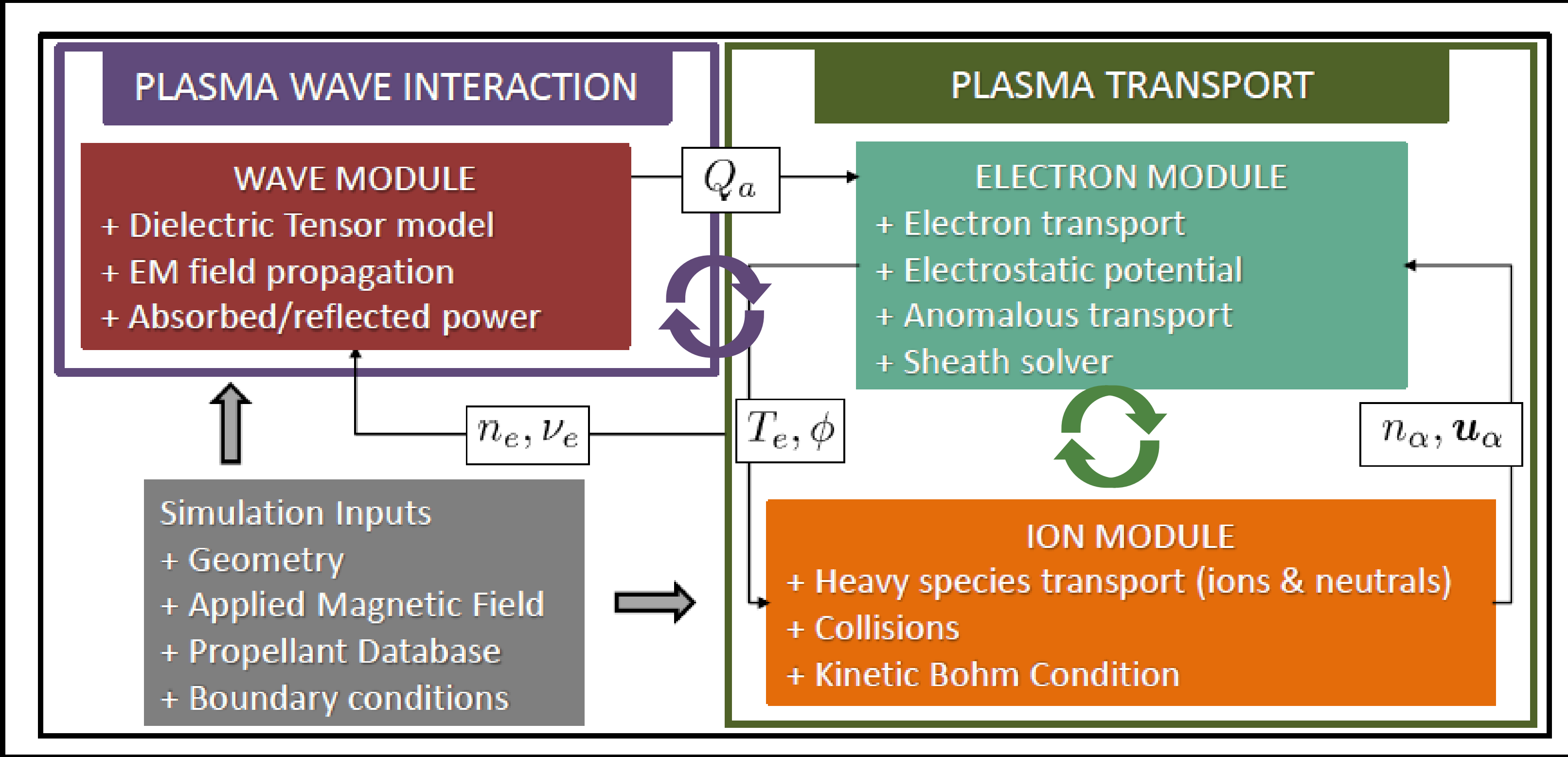

uc3m

A. Sánchez-Villar, J. Zhou, E. Ahedo, and M. Merino. Coupled plasma transport and electromagnetic wave simulation of an ECR thruster. *Plasma Sources Science and Technology 30 (2021) 045005.*

- Validation campaign carried out at ONERA facilities
- Dielectric-coated ECRT

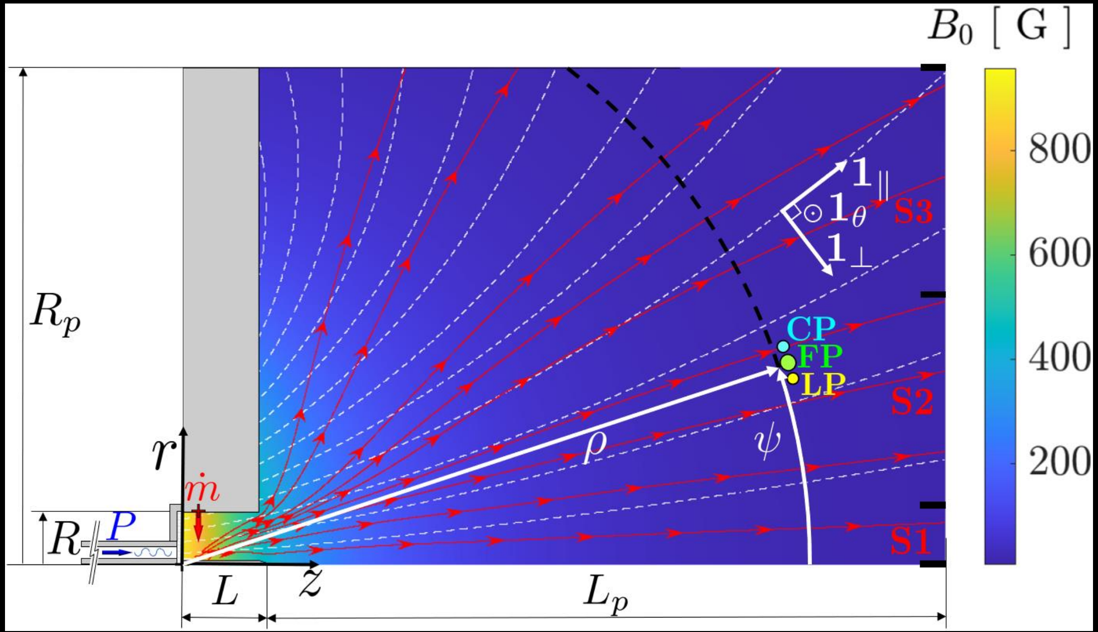

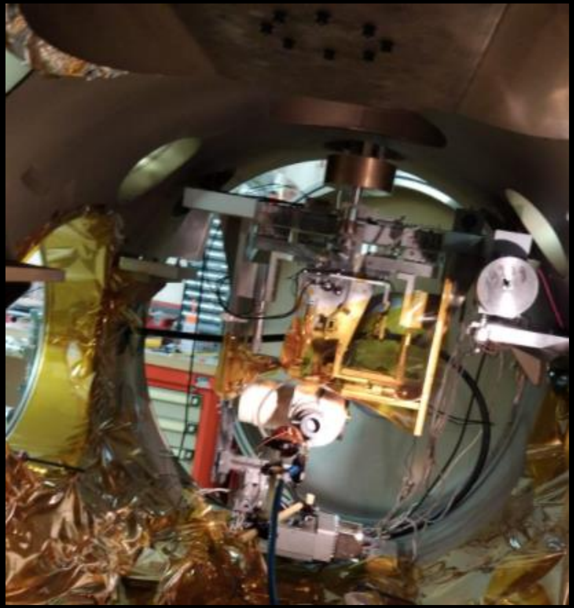

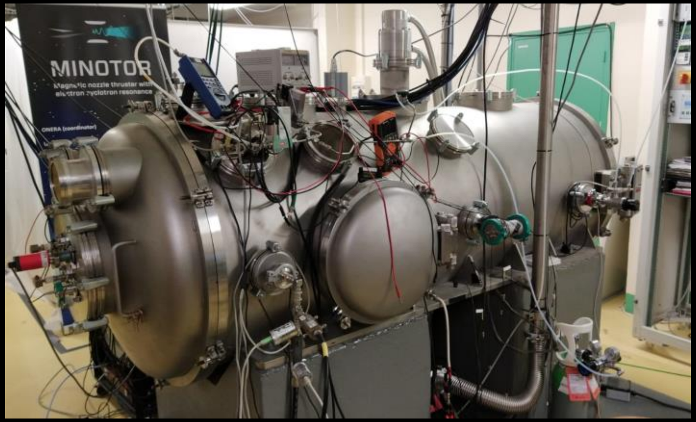

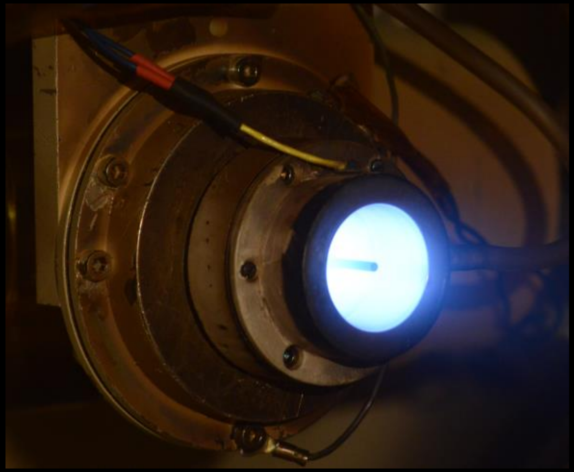

COMPARISON TO EXPERIMENTS

- Good agreement with experimental results along the magnetic nozzle

ANGULAR

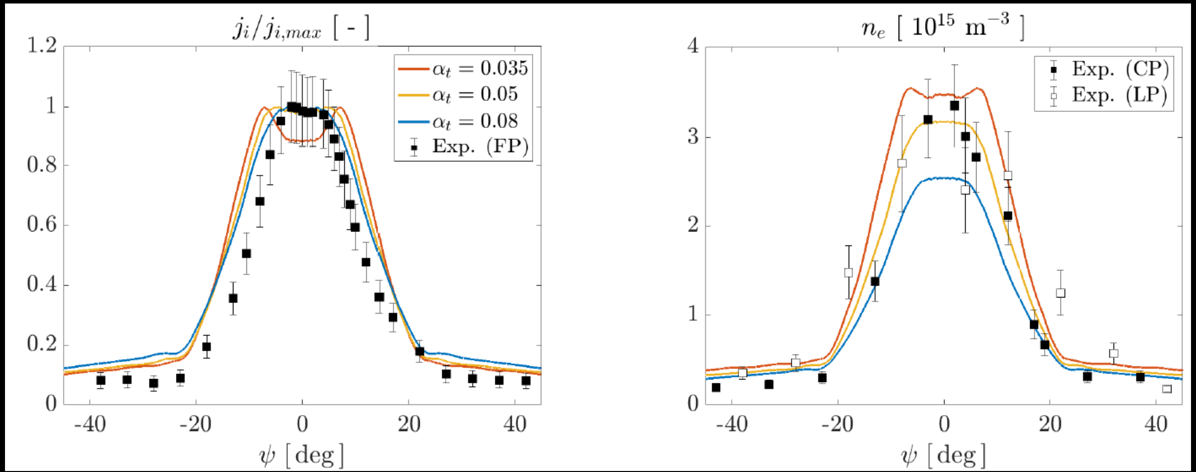

AXIAL

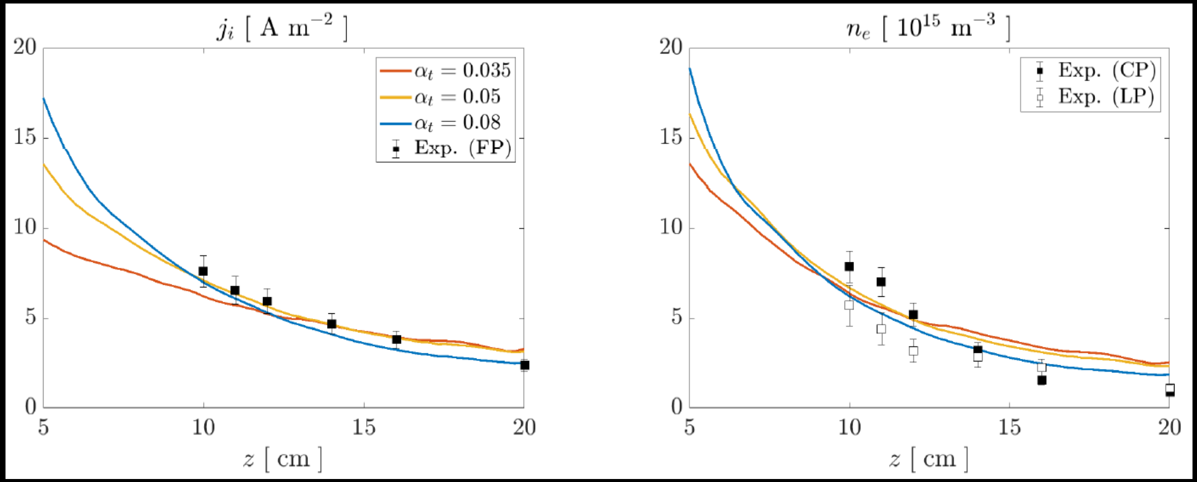

uc3m

MINOTOR

Magnetic nozzle thruster with electron cyclotron resonance

ONERA

THE FRENCH AEROSPACE LAB

A. Sánchez-Villar, F. Boni, V. Desángles, J. Jarrige, D. Packan, E. Ahedo & M. Merino. Comparison of a hybrid model and experimental measurements for a dielectric-coated coaxial ECR thruster. *Submitted to Plasma Sources Science and Technology (2022).*

Petra-M Simulations

- Petra-M: 3D + HPC capabilities

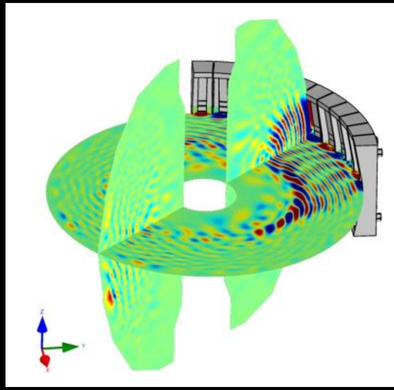

- Preliminary E-field solution with uniform tetrahedral mesh, ND elements order 2. Further refinement required in resonances.

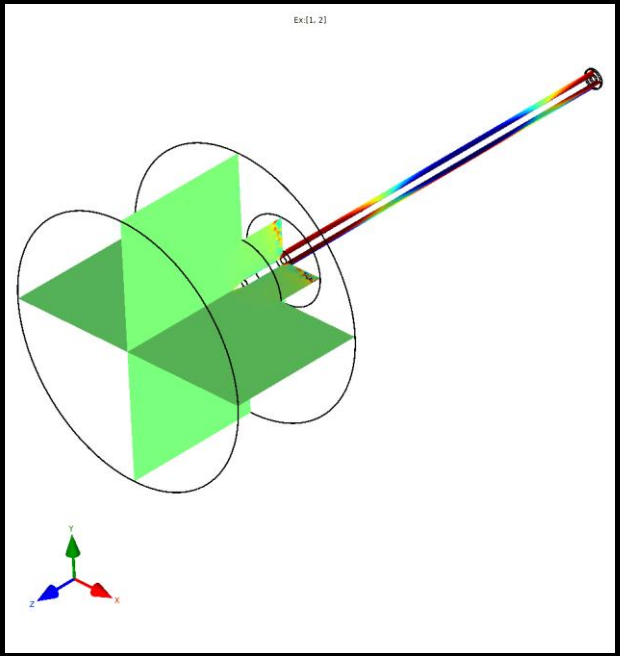

- Predictive mesh refinement based on estimated characteristic wavelengths depending on EM plasma regions

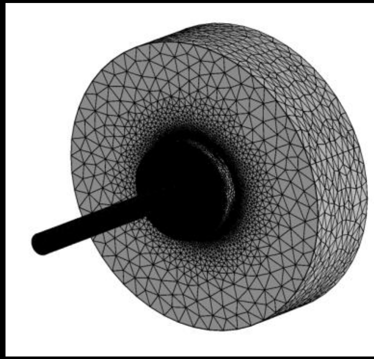

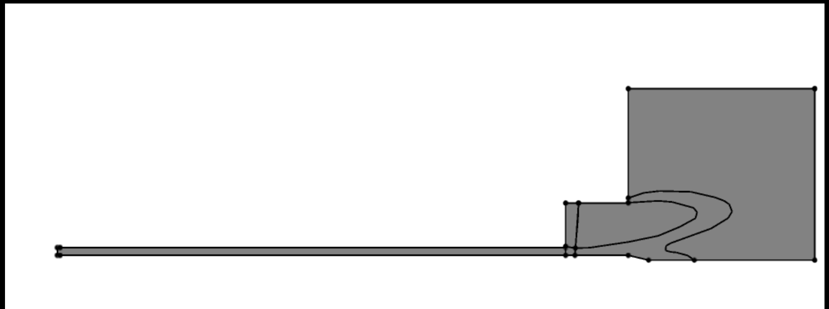

CONCLUSIONS

- Direct application of MFEM to the modeling of space plasma thrusters.
- 2D axisymmetric electromagnetic simulation code based on mixed finite elements
  - capable of solving the electromagnetic wave propagation and absorption in ECRT plasmas
  - Predictive mesh refinement based on the plasma and magnetic properties.
- Allowed to obtain:
  - First coupled simulations of an ECRT by coupling plasma transport and electromagnetic problems.
  - First validation of the model against experiments of benchmark ECRT prototype at ONERA
  - Good agreement between simulations and experiments and also to identify potential model improvements.
- Petra-M allows for the obtention of solutions efficiently and with 3D capabilities, crucial for non-axisymmetric thruster configurations.

THANK YOU!

mfem

uc3m

ONERA
THE FRENCH AEROSPACE LAB

PPPL

MINOTOR
Magnetic nozzle thruster with
electron cyclotron resonance